Preparation of a scaffold from (nano) hydroxyapatite-zirconium by sol-gel technique and evaluate its physical properties.

Jareonporn Saekhow[1*], Jasadee Kaewsrichan[2] and Lupong Kaewsichan[1]

[1]Department of Chemical Engineering, Faculty of Engineering, Prince of Songkla University, Hat-yai, Songkhla, 90112, Thailand
[2]Department of Pharmaceutical Chemistry, Faculty of Pharmaceutical Sciences, Prince of Songkla University, Hat-yai, Songkhla, 90112, Thailand
E-mail: Jareon.s@hotmail.com*

Abstract

Nano-hydroxyapatite (nHA) was prepared by sol-gel method using $Ca(NO_3)_2$ and $(HN_4)_2HPO_4$ as starting reagents. The synthesized nHA was separately blended with ZrO_2 at a mole ratio of 0.01, 0.1 and 0.5, respectively named as HA-0.01ZrO_2, HA-0.1ZrO_2 and HA-0.5ZrO_2. Scaffolds were fabricated by dipping and then sintering at either 1150 or 1250 °C for 2 h. X-ray diffraction (XRD) and Fourier transformed infrared (FTIR) spectroscopy techniques were utilized to characterize the prepared HA-ZrO_2 composites powders. It found that the addition of ZrO_2 causes an increase in the content of tricalcium phosphate, which hydroxyapatite phase has transformed into β-tricalcium phosphate. Furthermore, SEM evaluations showed the addition of ZrO2 particles reduces the size of HA grains and the pores are also smaller. The HA-ZrO_2 scaffolds were sintered 1250 °C for 2 h, the grain coalescence occurs densification more than more than sintering at 1150 °C and it gave the more forming apatite layers than sintering at 1150 °C too.

Keywords: hydroxyapatite, zirconia, sol-gel, tissue engineering, nano-particles

1. Introduction

Hydroxyapatite (HA) has drawn worldwide attention as an important substitute material in orthopedics and dentistry because of its biocompatibility, bioactivity and osteoconductivity, due to the chemical and biological similarity of this material to the mineral constituent of human bone [1,2,3,4]. However, the mechanical properties of HA are poor, it unsuitable for load-bearing applications and the application of bulk HA as the replacement for bone is thus limited [2,5]. Hence, To improve the mechanical properties of HA has thus attracted wide attention. One of the many approaches employs second-phase ceramic materials as the reinforcement to HA [5, 6].

An effective reinforcing agent for a ceramic–matrix composite material acts under specific conditions. First, the strength of the reinforcing phase must be higher than that of the matrix. Second, the interfacial strength between the matrix and the reinforcing phase should be neither too weak nor too strong. In the case of biomaterials, the biocompatibility of the second phase is another important factor that should be considered [7].

For HA reinforcement, ceramics such as zirconia, it is a widely used ceramic with favorable mechanical properties such as high bending strength and fracture toughness. These characteristics are considered to be comparable to those of natural bones. Owing to the high strength and stress-induced phase transformation toughening, it is frequently used to reinforce other ceramics [8]. This is results to use the zirconia as reinforcement.

Sintering HA at high temperatures can result in the formation of calcium phosphate based decomposition products such as tetracalcium phosphate [TTCP] $\{Ca_4(PO_4)_2O\}$ which can further degrade to tri-calcium phosphate [TCP] $\{Ca_3(PO_4)_2\}$ and calcium oxide [CaO]. These secondary phases have, in certain instances, been reported to adversely affect biological response [9]. However, it has been reported that the addition of ZrO_2 causes an increase in the content of tricalcium phosphate (β-TCP, $Ca_3(PO_4)_2$), which seriously deteriorates the mechanical properties and chemical stability of these composites [2].

In order to obtain a HA–YSZ composite have superior mechanical properties. In this work, The aim of the present study was to prepare HA-ZrO_2 composite nano-powders, the optimum sintering temperature and the effect of the ZrO_2 addition on the microstructure evolution during sintering is investigated.

2. Materials and methods

2.1. Synthesis of HA

The flow chart show in Fig. 1 outline the experimental procedure used to generate the HA powder described in this study. Calcium nitrate tetrahydrate ($Ca(NO_3)_24H_2O$) (Carlo Erba Reagents)

and Diammonium phosphate $(NH_4)_2HPO_4$) (Carlo Erba Reagents) were used as starting calcium and phosphorous. Ammonium hydroxide (NH_4OH) (J.T. Baker) was used for adjusting the pH of the solution and nitric acid (HNO_3) (March) was dissolved precipitate in solution. Preparation of 1 M $Ca(NO_3)_24H_2O$ and 0.67 M $(NH_4)_2HPO_4$ was made by dissolving the crystals in deionized water. The $(NH_4)_2HPO_4$ solution was added dropwise to the $Ca(NO_3)_24H_2O$ solution while stirring at 65 °C and the mixture was continuously stirred for about 24 h at ambient temperature. Before mixing, nitric acid was added dropwise to obtain white transparent solution , the pH value of the solution was adjusted above 11 with NH_4OH.

The powder products were obtain by filtering the solutions. The filtered products were repeatedly washed, dried at 65 °C. This dried powder was calcined at 900 °C for 4 h in electrical furnace in air.

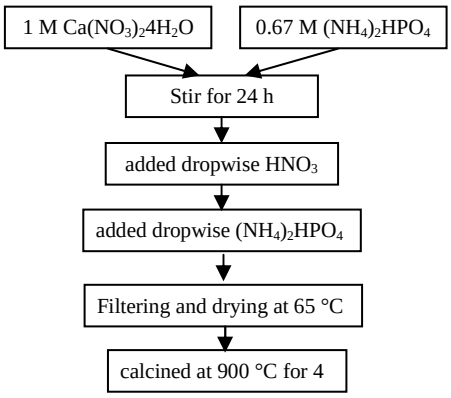

Figure 1. Schematic flow chart showing the sol-gel procedure for synthesizing HA.

2.2 Preparation of composite powders and fabrication of scaffold.

The mixed composite powder containing synthesis of HA and zirconia (ZrO_2) (Riedel-de Haen) with mol ratios in table 1.

Table 1 Compositional ratio of HA and ZrO_2 in composite powder.

Formula	ZrO_2/HA mol ratio
HA-0.01ZrO_2	0.01
HA-0.1ZrO_2	0.1
HA-0.5ZrO_2	0.5

The composite powder slurry was prepared using 1% PVA as a binding solution. The luffa templates with appropriate dimensions were dipping into the slurry until completely coated. The coated templates were sintered at 1150 °C or 1250 °C for 2 h.

3. Results and discussion

3.1 characterization of synthesis HA

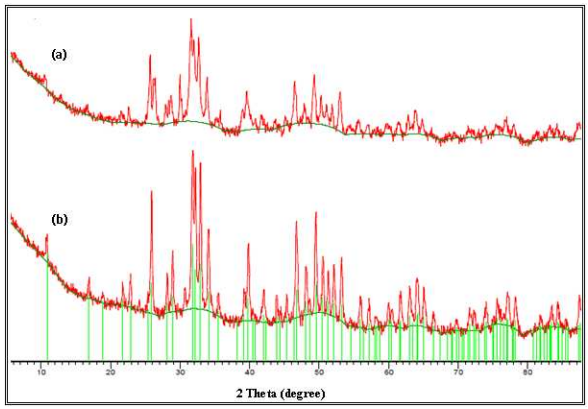

Figure 2. XRD patterns of HA (a) and calcined HA powders at 900 °C for 4 h (b).

Fig. 2 shows the XRD pattern of and calcined HA powders at 900 °C for 4 h. XRD patterns of HA powders at 900 °C powders showed no presence of secondary phases indicating that the final product was of high purity. EDX analysis of synthesized HA powders at 900 °C showed calcium and phosphorus exhibiting a ratio (Ca/P) of 2.26. Thus, synthesis HA was used prepare HA-ZrO_2 composites.

3.2 characterizations of HA-ZrO_2 composites.

Thermal analysis, It is well specified that temperature control during the synthesis is crucial to influence the reaction progress and the properties of the HA–YSZ composite. Thus, the thermal decomposition mechanism of the HA-ZrO_2 composite was studied by TGA measurements [7].

TGA curves of the HA-ZrO_2 composites powders are given in Fig. 3 (a-d). The total weight losses observed were about 1.67%, 1.47%, 1.70%, and 1.06% for synthesis HA, HA–0.01 ZrO_2, HA–0.1 ZrO_2, and HA–0.5 ZrO_2 composite, respectively, in the temperatures range of 50–1300 °C. The weight loss in the region of 140–700 °C is due to the evaporation of adsorbed, chemisorbed water molecules and Contamination. The onset temperature in second decomposition step , it observed were about 815.00, 838.98, 895.35 and 785.28 for systhesis HA, HA–0.01ZrO_2, HA–0.1ZrO_2, and HA–0.5ZrO_2 composite, respectively. This can be attributed to the partial decomposition of hydroxyapatite into oxyapatite that , in turn, converts into tricalcium phosphate (TCP) [10]. These processes are corroborated by the observations made XRD analyses.

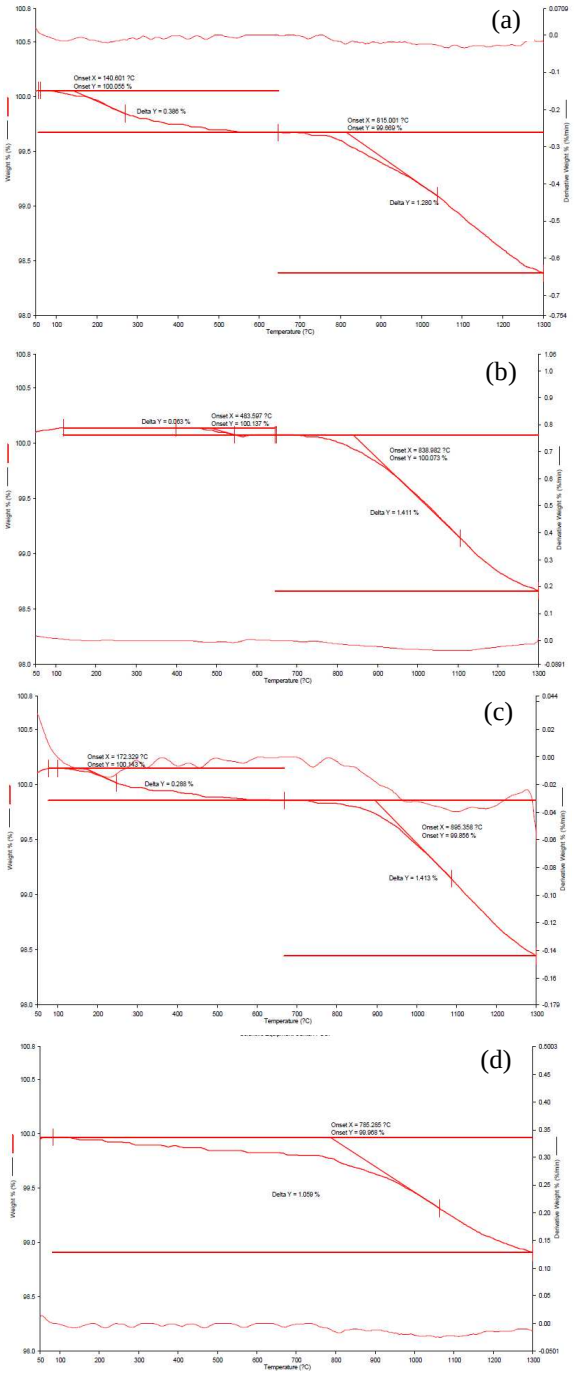

Figure 3. Typical TGA curves of (a) synthesis HA (b) HA-0.01ZrO_2 (c) HA-0.1ZrO_2 and (d) HA-0.5ZrO_2 composite.

XRD patterns in Fig. 4 shown the most intense X-ray diffraction peaks of the synthesis HA and HA-ZrO_2 composites present HA, β-tricalcium phosphate ($Ca_3(PO_4)_2$) and zirconium oxide (ZrO_2) also HA-0.5ZrO_2 composite has the peaks correspond to baddeleyite too. The intensities of the β-tricalcium phosphate peaks with increases as the amount of zirconium oxide increases. This indicates that some hydroxylapatite phase has transformed into β-tricalcium phosphate (whitlockite) [3,11,12] and the addition of ZrO_2 causes an increase in the content of tricalcium phosphate [2,9]. In the HA-0.5ZrO_2 composite, some zirconium oxide phase (tetragonal phase) has transformed into baddeleyite (monoclinic phase [2].

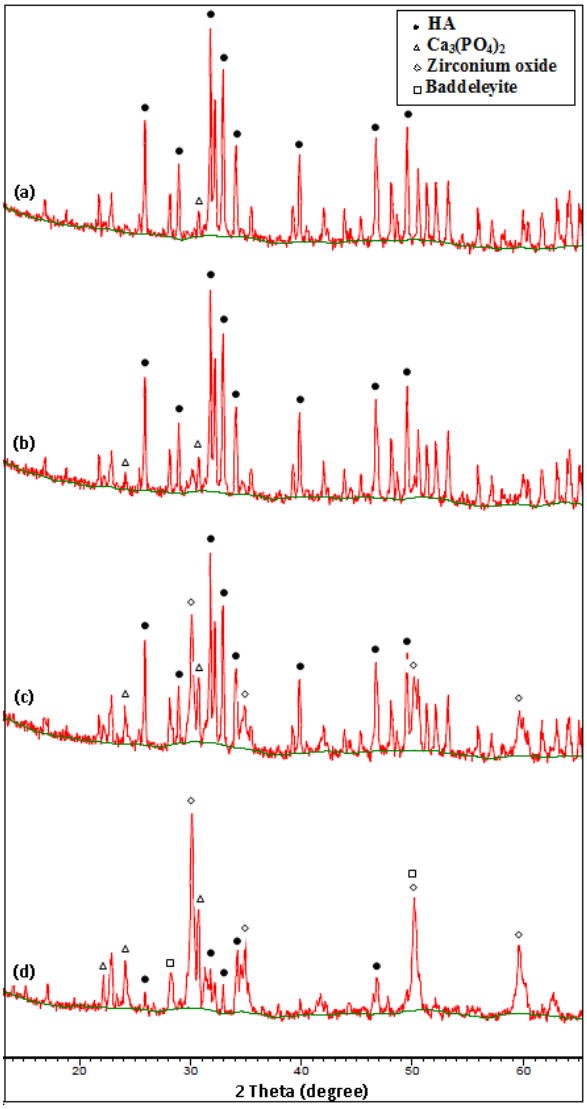

Figure 4. XRD patterns of (a) systhesis HA (b) HA-0.01ZrO_2 (c) HA-0.1ZrO_2 and (d) HA-0.5ZrO_2 composites after sintering at temperature of 1250 °C for 2 h.

As shown in the FTIR spectra (Fig. 5), the band at 3575 cm^{-1} belong to hydroxyl vibration. These spectra indicate the formation of a HA structure containing sharp O-H and P-O bands. The band at 575 cm^{-1} is the typical bands of phosphate bending vibration, while the band at 1059 cm^{-1} are due to phosphate stretching vibration [4,7,13]. FTIR spectra of the HA-0.01ZrO_2 and HA-0.1ZrO_2 composites show the absorption bands characteristic of hydroxyapatite, together with O-H and P-O bands. On the other hand, FTIR analysis of HA-0.5ZrO_2 composite powder indicates that the O-H absorbance

band of 3575 cm^{-1} disappears. This confirms that some hydroxyapatite phase has transformed into β-tricalcium phosphate.

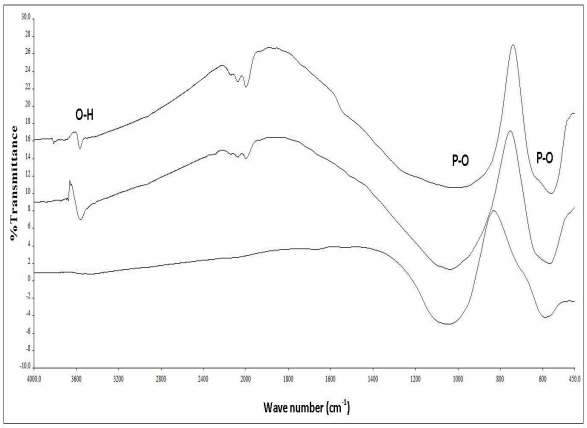

Figure 5. FTIR spectra of the (a) HA-0.01ZrO_2 (b) HA-0.1ZrO_2 and (c) HA-0.5ZrO_2 composites after sintering at temperature of 1250 °C for 2 h.

3.3 physical properties of scaffold

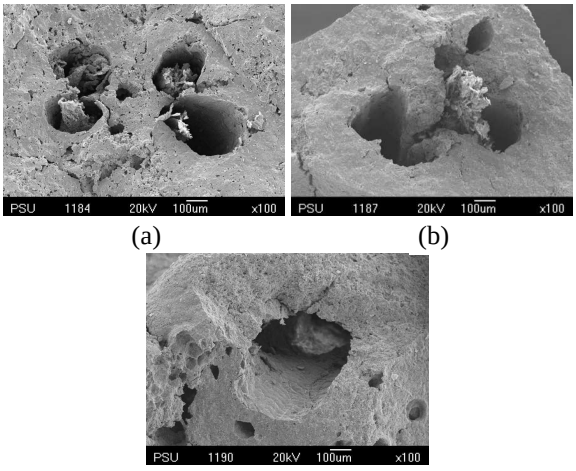

(a) (b)

(c)

Figure 6. SEM micrographs of HA-ZrO_2 scaffolds (a) HA-0.01ZrO_2 (b) HA-0.1ZrO_2 and (c) HA-0.5ZrO_2

Fig. 6 shows the SEM images of the pores are formed by the space left by the luffa's fiber eliminated during the sintering. It measuring in the range 214.29 to 400 µm. This pore is connected by others in a way that all ceramic fibers of the reticulated ceramic have a similar channel in its interior, creating a network of the channels inside the network of the ceramic fibers.

Fig. 7 shows the average size of HA grains in the both sintered composites as a function of ZrO2 content. The addition of ZrO2 particles reduces the size of HA grains. Furthermore, the pores are also smaller, indicating that the presence ZrO2 particles effectively pin the grain boundaries of the HA matrix and prevent complete densification [5,9]. In additional, sintering temperature at 1250 °C, grain coalescence occurs densification more than sintering temperature at 1150 °C [14].

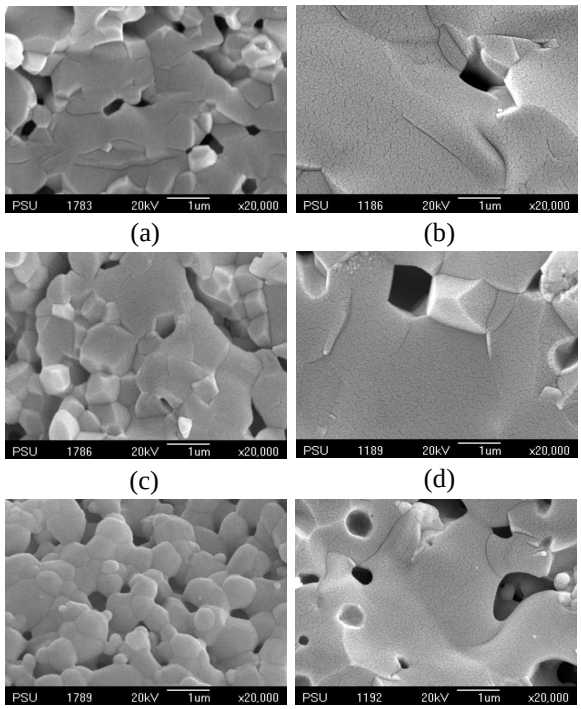

(a) (b)

(c) (d)

(e) (f)

Figure 7. SEM morphologies of HA-ZrO_2 scaffolds (a) HA-0.01ZrO_2 (c) HA-0.1ZrO_2 (e) HA-0.5ZrO_2 sintered at 1150 °C and (b) HA-0.01ZrO_2 (d) HA-0.1ZrO_2 (f) HA-0.5ZrO_2 sintered at 1250 °C for 2 h.

Fig. 8 showed the morphology of the apatite layer. At the same time, the sintering temperature at 1250 °C gave the more forming apatite layers than sintering temperature at 1150 °C. The sintering temperature at 1250 °C, maggot-like apatite formations were visible at grain boundaries. On the other hand, the sintering temperature at 1150 °C, sphere-like apatite formations were visible on surface of grain.

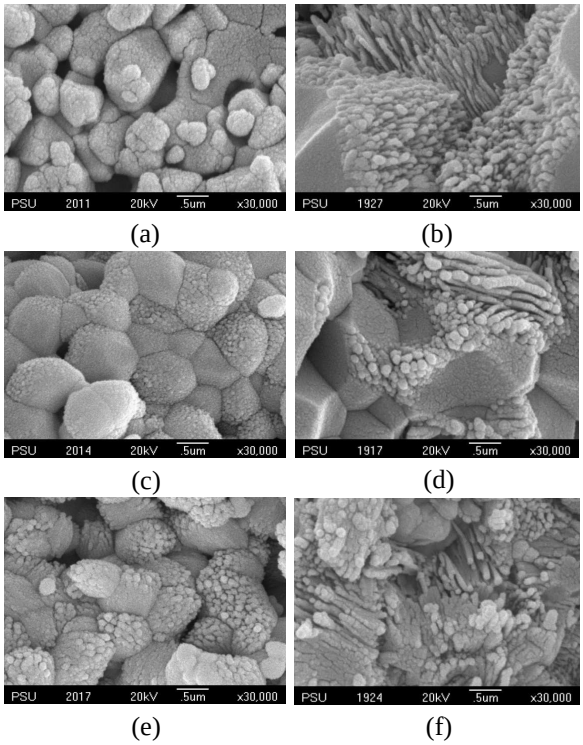

Figure 8. SEM morphologies of HA-ZrO_2 scaffolds (a) HA-0.01ZrO_2 (c) HA-0.1ZrO_2 (e) HA-0.5ZrO_2 sintered at 1150 °C and (b) HA-0.01ZrO_2 (d) HA-0.1ZrO_2 (f) HA-0.5ZrO_2 sintered at 1250 °C for 2 h and soaked in PBS for 3 day.

4. Conclusion

The preparation of HA-ZrO_2 scaffolds, the addition of ZrO_2 causes an increase in the content of tricalcium phosphate, which hydroxyapatite phase has transformed into β-tricalcium phosphate. Furthermore, The addition of ZrO2 particles reduces the size of HA grains and the pores are also smaller. The HA-ZrO_2 scaffolds were sintered 1250 °C for 2 h, the grain coalescence occurs densification more than more than sintering at 1150 °C and it gave the more forming apatite layers than sintering at 1150 °C too.

Acknowledgments

The authors gratefully acknowledged the financial supports from the Graduate School of Prince of Songkla University and Discipline of Excellence (DoE) in Chemical Engineering Prince of Songkla University.

References

[1] Zamani, A.H., Behnamghader, A. and Kazemzadeh, A. 2008. Synthesis of nanocrystalline carbonated hydroxyapatite powder via nonalkoxide sol–gel method. Materials Science and Engineering, C28:1326–1329.

[2] Vasconcelos, H.C. and Barreto, M.C. 2010. Tailoring the Microstructure of Sol–Gel Derived Hydroxyapatite / Zirconia Nanocrystalline Composites. Nanoscale Res Lett, DOI 10.1007/s11671-010-9766-z.

[3] Fathi, M.H. and Hanifi, A. 2007. Evaluation and characterization of nanostructure hydroxyapatite powder prepared by simple sol–gel method. Materials Letters, 6: 3978–3983.

[4] Lee, Kim and Cho. 2009. Sol–gel synthesis and characterization of hydroxyapatite nanorods. Particuology, 7: 466–470.

[5] Chiu, Hsu and Tuan. 2007. Effect of zirconia addition on the microstructural evolution of porous hydroxyapatite. Ceramics International, 33: 715–718.

[6] Rao, R. and Kannan, T.S. 2002. Synthesis and sintering of hydroxyapatite–zirconia composites. Materials Science and Engineering, C20:187–193.

[7] Salehi, S. and Fathi, M.H. 2010. Fabrication and characterization of sol–gel derived hydroxyapatite/zirconia composite nanopowders with various yttria contents. Ceramics International, 36: 1659–1667.

[8] Xie, Liu, Zheng , Ding and Chu. 2006. Improved stability of plasma-sprayed dicalcium silicate/zirconia composite coating. Thin Solid Films, 515: 1214–1218.

[9] Curran , Fleming, Towler and Hampshire. 2010. Mechanical properties of hydroxyapatite–zirconia compacts sintered by two different sintering methods. J Mater Sci: Mater Med, 21:1109–1120.

[10] Velu and Gopal. 2009. Preparation of Nanohydroxyapatite by a Sol–Gel Method Using AlginicAcid as a Complexing Agent. J. Am. Ceram. Soc., 92 [10]: 2207–2211.

[11] Ming and Sheng. 1988. Sintering of hydroxylapatite-zirconia composite Materials. Journal of materials science, 23: 3771- 3777.

[12] Evis. 2007. Reactions in hydroxylapatite–zirconia composites. Ceramics International, 33: 987–991.

[13] Kim and Kumta. 2004. Sol–gel synthesis and characterization of nanostructured hydroxyapatite powder. Materials Science and Engineering, B 111:232–236.

[14] Assollant, D., Ababou, A., Champion, E. and Heughebaert, M. 2003. Sintering of calcium phosphate hydroxyapatite $Ca_{10}(PO_4)_6(OH)_2$ I. Calcination and particle growth. Journal of the European Ceramic Society, 23: 229–241.